

# Resettable Land Anchor Launcher for Unmanned Rover Rescue and Slope Climbing

Aaryan Kainth<sup>1</sup>, Andrew R. Krohn<sup>1</sup>, Kyle Johnson<sup>2</sup>, Alexander Schepelmann<sup>2</sup>, Elliot W. Hawkes<sup>3</sup>,  
and Nicholas D. Naclerio<sup>3\*</sup>

**Abstract**—Unmanned planetary rovers have traversed kilometers of Lunar and Martian terrain while performing valuable science. However, they still face mobility challenges including steep slopes and unstable soil that can entrap vehicles, as demonstrated by NASA’s Spirit rover. Vehicles on Earth can depend on a human operator or rescue vehicle to tow them out of an entrapment, but remote rovers cannot, limiting their route to highly conservative path selections. To increase rover mobility on slopes and unstable soils, we present a resettable anchor launcher for independent self-rescue. The device launches a tethered land anchor away from the rover and then uses a winch to tow the rover up a hill or out of an entrapment. This paper presents the design of the launcher and its integration into a half-meter-long rover mobility platform with field testing at the NASA Glenn Research Center SLOPE Lab. We demonstrate repeatable launching and winching to help the rover climb a 17° slope of loose GRC-1 Lunar regolith simulant that it otherwise could not climb. Our work presents an alternative method to increase rover mobility, especially up slopes, and enables independent rover rescue, which could eventually increase mission duration and reduce risk of entrapment during extraterrestrial exploration.

## I. INTRODUCTION

Unmanned planetary rover mobility platforms (hereafter referred to as “rovers”) have been successfully executing missions since the early 1970’s on the Moon [1], and late 1990’s on Mars [2]. While there have been many successful missions, rovers still struggle with obstacles such as soft soils and slopes as low as 17° [3]. This can impede movement and limit mission success, and in the worst case cause mission-ending entrapment such as what happened to NASA’s Spirit rover [4].

Numerous studies that focus on wheel and suspension design have been conducted to improve traction and mobility [5]. Although most designs have prioritized reliability, efficiency and durability, systems like NASA’s VIPER rover [6] (and others [7], [8], [9], [10], [11]) have explored more complicated active independent suspension with complex crawling wheeled gaits. The mobility of these rovers is increased at the cost of complexity, such as additional actuators and degrees of freedom on each wheel, which may be impractical for some systems.

This work was partially supported by an Early Career Faculty grant from NASA’s Space Technology Research Grants Program.

<sup>1</sup>College of Engineering, University of California, Santa Barbara, CA 93106.

<sup>2</sup>NASA Glenn Research Center, Cleveland, OH 44135

<sup>3</sup>Department of Mechanical Engineering, University of California, Santa Barbara, CA 93106.

\*Corresponding author. Email: nicholas.naclerio@gmail.com



Fig. 1. The anchor launcher mounted on a rover mobility platform to help climb a 17° slope of loose regolith simulant at the NASA Glenn Research Center SLOPE Lab. For scale, the rover wheel base is 57 cm long.

Other creative mobility concepts have involved tethered systems to lower part of a rover down a steep slope [12], [13], [14], or wrap a tether around natural objects [15]. These solutions center around changing the form of the rover itself, usually by adding a second or third robot to act as a tethering point. Such systems require prior planning at the top of a slope, and do not help a rover that has already become entrapped.

To address the challenges of entrapment and climbing slopes, we introduce a self-rescuing anchor launcher for extraterrestrial rovers. After launching an anchor up a hill, the rover can use it as a tether point to winch itself up, similar to a truck on Earth winching against a tree to pull itself free from mud. This launcher improves mobility on steep, soft-soil terrain, enabling rovers to conduct operations in previously inaccessible places and enhance mission longevity.

Grapple, harpoon, and anchor launchers are not a new invention; however, to our knowledge, the mechanism in this paper is the first system for rover mobility purposes, and the first launcher for mobile robotic applications that can automatically deploy and reset repeatedly. The most similar concept to our design is a spring loaded launcher that deploys a marine anchor from the beach to measure surf conditions [16]. Other one-time use launchers have been designed for space applications other than rovers, such as harpooning space junk [17] and asteroid sampling [18].

This paper presents the design and fabrication of the anchor launcher prototype and its ability to help a lightweight



Fig. 2. The anchor, on the left, connected by the winch string to the launcher, on the right.

rover climb a  $17^\circ$  slope of lunar regolith simulant that it otherwise could not climb (Fig. 1). A video of the launcher’s operation can be viewed on YouTube [19].

## II. DESIGN AND FABRICATION

### A. Working principle

The strategy of the anchor system developed in this paper is to launch a land anchor away from the rover and use it as a tether to winch the rover up a slope or out of an entrapment. The launcher is composed of 5 main components: 1) the anchor which digs into the ground to provide a point to winch from, 2) the launcher to propel the anchor away from the rover, 3) the winch to both wind up the launcher and tow the rover, 4) a release and reset mechanism to enable repeatable anchor launches, and 5) a mount to attach to the rover.

### B. Anchor

Two anchor designs were explored, one radially asymmetric and one radially symmetric. The symmetric design was included only for launch testing, but was not optimized for anchoring in sand. As such, only the asymmetric anchor was tested on the rover.

The asymmetric anchor is a modified nylon plough style kayak anchor attached to a 6.4mm diameter aluminum rod to interface with the anchor launcher (Fig. 2). Its weighted tip causes it to roll upright from any orientation (total mass = 250g). Its anchoring force changes depending on the angle at which it is pulled: when pulled parallel to the ground, it provides a strong anchoring force, but when pulled perpendicular to the ground, the anchor is easily dislodged (see Sec. IV-C). A braided fishing line is attached to the end of the rod and connected at the other end to the winch.

### C. Launcher

The spring-loaded launcher consists of four major components marked in Fig. 2 that allow it to repeatably launch the anchor: a frame, a mobile carriage, springs, and a flared barrel. In total, the anchor launcher and the winch and trigger release mechanism (next section) have a mass of 543 grams.

The frame is made from two aluminum L-bracket rails bolted to 3D printed brackets. The 3D printed mobile carriage slides along the frame rails, transferring force from the launcher to the anchor. It has a tapered hole in its center for the winch line to pass through from the winch to the anchor. As the winch pulls the anchor into the launcher, the end of the anchor rod seats in the carriage and pulls back on the launcher springs as shown in Fig. 4.

Two tensile coil springs are attached between the frame and mobile carriage to store energy to launch the anchor.

The flared barrel at the end of the launcher guides the anchor back into the launcher when resetting. A 5 cm long, 1 cm inner diameter carbon fiber tube is adhered to the inside of the barrel to prevent jamming and guide the anchor into the mobile carriage when resetting.

### D. Winch and trigger release

The winch and trigger shown in Fig. 3 serve to both tow the rover and wind-up and release the launcher. The system is inspired by the quick unspooling behavior of a spinning reel for fishing combined with the high force trigger release used on a spring loaded jumping robot [20].

The winch is driven by a 12V DC gear motor oriented parallel to the launcher frame as shown in Fig. 3A. When the trigger is released (Fig. 3B) the winch line quickly unspools off the end of the winch without needing to rotate the winch.

The trigger prevents the winch line from unspooling until ready. There is a free-spinning roller on one side of the latch which the winch line slides past as it winds on the winch. One end of the latch is pinned to the 3D printed winch frame, while the other side is held in place by a release trigger (Fig. 3A). As the trigger is pulled away on command by a small release motor, the tension of the winch line pulls the latch free and the line unspools (Fig. 3B). The amount that the winch is spooled and the launcher springs stretched is controlled by the winch motor, and can be released at any point by the trigger release motor. This means that the anchor launching distance can be varied as desired.

TABLE I  
NOTES ON MATERIALS AND ITEMS USED

Material or Item	Note
Anchor head	“230g nylong kayak anchor,” Cooper Anchors
3D printer filament	MarkForged Onyx Nylon
Winch motor	37mm diameter, Greartisan
Release motor	Pololu micro-metal gear motor
Winch line	65-lb test Spectra

### E. Reset mechanism

After the anchor has launched and been used to tow the rover, it is pulled out of the ground and back into the launcher by the winch.

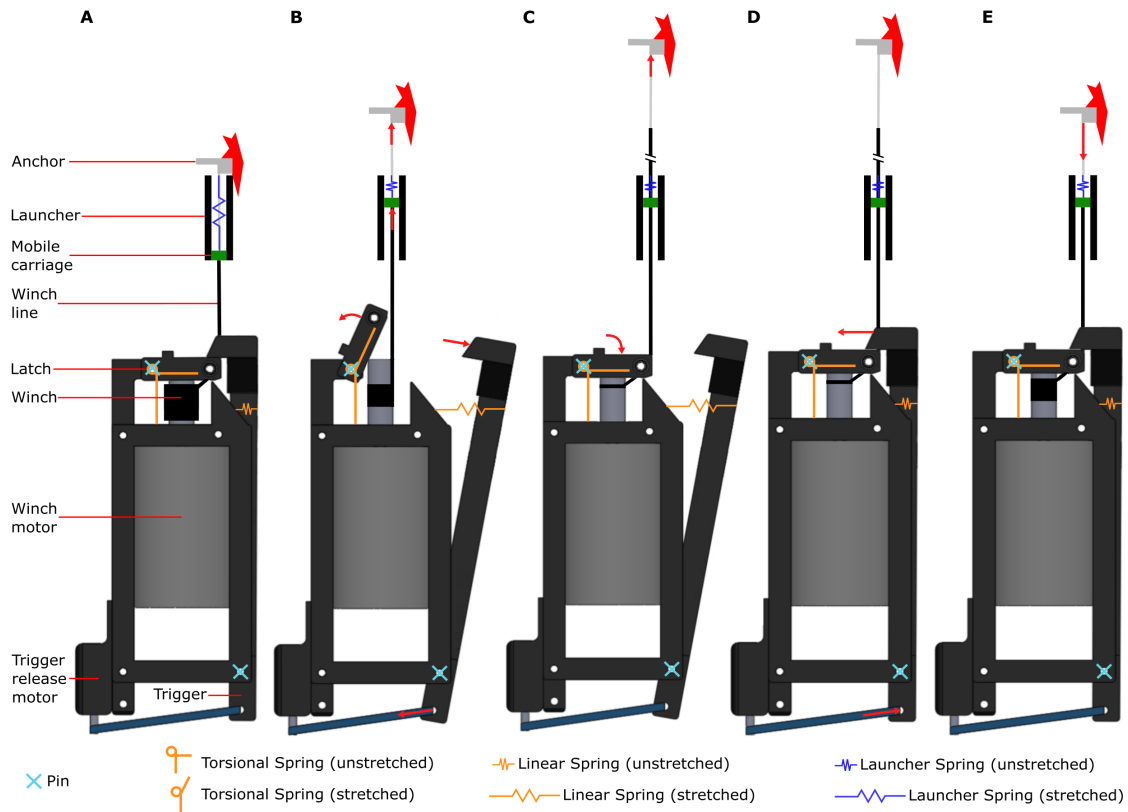


Fig. 3. The launching process in five steps (not to scale). Red arrows represent motion just before the indicated step. A) The latch is in its closed position, and the winch has been spooled to its full extent, stretching the launcher spring and readying the anchor for launch. B) The trigger release motor on the bottom left spins, pulling the bottom of the latch and causing it to open. The arm attached to the torsional spring swings open, propelled by the tension in the winch line from the force of the launcher springs. The anchor is launched by the force of the launcher springs, which is directed through the mobile carriage. C) The launch has finished, and little to no winch line is left on the spool. The latch is held open, allowing the torsional spring to reset the arm. D) The trigger release motor spins in reverse, allowing the linear spring to reset the latch. The system is now ready to tow the rover by running the winch motor. E) The winch has towed the rover up to the anchor, and the system is ready to reset the launcher by running the winch motor.

The spring loaded latch automatically returns to its closed position (Fig. 3C). The trigger motor is then released to close the trigger and secure the latch (Fig. 3D). This allows the winch to tow the rover (Fig. 3E) and then wind up the launcher again as shown in Fig. 4. It is important to note that the launcher springs are unaffected by winching up until the point at which the anchor rod makes contact with the mobile carriage on the launcher; the tension from winching is fully directed into pulling the rover uphill.

#### F. Integration with rover

To demonstrate the utility of the resettable anchor launcher, we integrated it with a simple, wireless rover platform.

The lightweight rover demonstrated in this paper was adapted from a commercial drone kit and consists of a carbon fiber frame, wireless controller, battery, and four servo driven wheels made of perforated aluminum sheet rims and wire spokes. The rover was remotely driven by skid steer and electrically integrated with the anchor launcher to control the winch and trigger release motors. The length and width of the rover wheel base are 53 cm and 57 cm respectively.

The launcher was attached to a carbon fiber spar out the

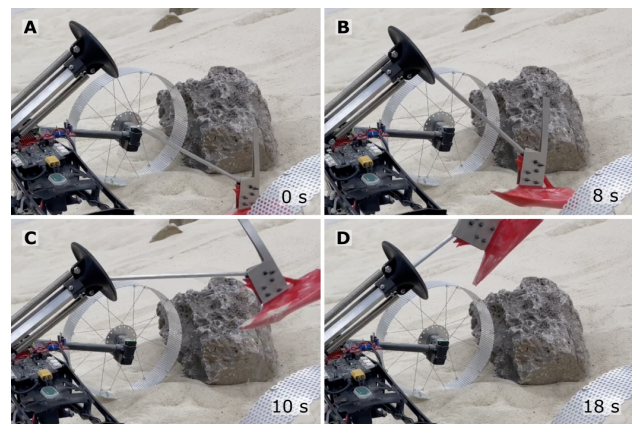


Fig. 4. The anchor automatically resetting into the launcher (A-D) by running the winch motor with the release mechanism closed (Fig. 3D) and then launching (E) by releasing the release mechanism (Fig. 3B).

back of the rover body, as shown in Fig. 5. The winch and trigger release motors were integrated into the rover's battery power supply and wireless control system, and controlled over Bluetooth.

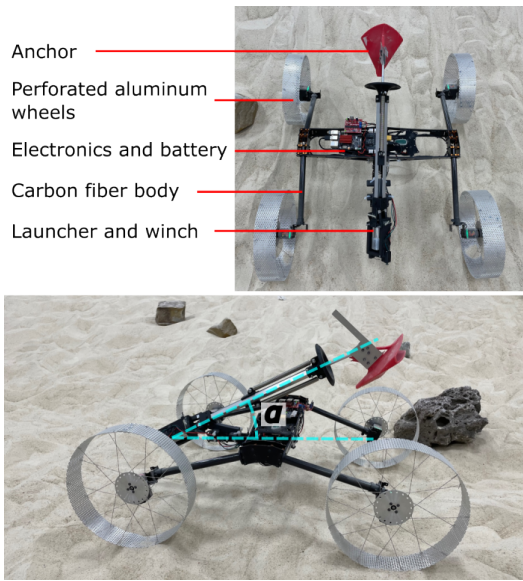


Fig. 5. Lightweight rover with integrated anchor launcher. Top: top view with major components labeled. Bottom: side view with angle of inclination ( $\alpha$ ) labeled. Length and width of wheel base are 53 and 57 cm respectively for scale.

A consideration for rover integration is the launcher angle of inclination  $\alpha$  (see Fig. 5) that maximizes launch distance up a slope of angle  $\beta$ . The expression  $\alpha = 45 - \frac{\beta}{2}$  [21] maximizes launch distance up a slope; thus, the optimal  $\alpha$  for a  $\beta = 17^\circ$  slope is  $36.5^\circ$ . Accordingly, the launcher was oriented at approximately this angle.

### III. MODELING

We include three simple models to help understand the behavior of the system and offer design insights. The first model considers the behavior of the anchor as it interacts with granular matter, to help explain why the angle of pull results in different pullout forces. The second model examines the energetics of the launch, and offers insights into which components should be modified to improve launch efficiency. It also informs the user how far back the spring should be pulled to launch a certain distance. The third model defines the net force on the attached rover, explaining how the anchor assists with slope climbing.

#### A. Anchor-soil Interaction Model

The angle-dependent interaction between anchor and soil can be modeled using granular resistive force theory [22], which works by summing the resistive forces on an object moving through a granular medium. In our case, we model the anchor as a flat plate at  $-22^\circ$  (the angle between the anchor wedge and its rod) from the angle of attack it is pulled from. The forces on it are estimated by interpolating published experimental resistance values in loose poppy seeds (SI in [22]) resolved for the angle of attack from horizontal to vertical. The forces are scaled linearly to match our highest force magnitude.

#### B. Energetics of Launch

For this analysis, we consider three main components: the anchor, the carriage, and the spring. We assumed that the spring has a linear gradient of velocity, and thus that two-thirds of the spring is static while the remaining third is in motion at the same velocity as its end [20]. In this analysis, we will refer to the summed mass of the anchor, carriage, and one third of the spring as  $m_{total}$  (i.e.  $m_{total} = m_{anchor} + m_{carriage} + \frac{1}{3}m_{spring}$ ). The winch line's specific mass is low ( $\approx 2 \times 10^{-4}$  kg/m), so we will disregard it.

A preliminary calculation of the drag force on the asymmetric anchor (assuming  $C_d = 1$ , and initial launch velocity) yielded a magnitude of 0.044 N, multiple orders of magnitude less than the gravitational force; we will thus assume that drag is negligible in changing trajectory, and disregard it for this analysis.

The springs in the presented launcher are preloaded, but otherwise linear; we can thus integrate under the force-distance curve over the pullback distance to get the stored energy to be  $U_{spring} = \frac{1}{2}k_s x^2 + cx$ , where  $k_s$  is the spring constant,  $x$  is the pullback distance of the spring, and  $c$  is the preloaded force value. If we assume some losses  $E_{loss}$  due to non-idealities, such as friction of the anchor as it leaves the launcher, we can write the kinetic energy of the anchor at launch as:

$$K_{anchor} = (U_{spring} - E_{loss}) \frac{m_{anchor}}{m_{total}}. \quad (1)$$

Assuming no losses, we can write the velocity at launch as:

$$v_0 = \sqrt{\frac{k_s x^2 + cx}{m_{total}}}. \quad (2)$$

We next model the distance the anchor would launch with velocity  $v_0$  at a given initial height  $y_0$ . Assuming an angle  $\theta$  that is the angle of the launcher with respect to the horizontal ground, and assuming no losses, we can write:

$$d = \frac{v_0 \cos \theta \left( v_0 \sin \theta + \sqrt{v_0^2 \sin^2 \theta + 2gy_0} \right)}{g} \quad (3)$$

(1) informs us that to increase the launch distance of the anchor, one should increase the proportion of kinetic energy that goes into it by decreasing primarily the mass of the carriage, and secondarily, the mass of the springs. (3) tells us how to control the launch distance of the anchor. An additional maximum constraint is set on  $d$  by the length of winch line loaded in the launcher. The parameters of the nominal system are listed in Table II.

TABLE II  
THE SPRING PARAMETERS AND MASSES OF THE SYSTEM

Parameter	Value
$m_{carriage} + \frac{1}{3}m_{spring}$	0.0353 kg
$m_{asymm\ anchor}$	0.25 kg
$m_{symm\ anchor}$	0.088 kg
$k_s$	$13.5 \frac{N}{cm}$
$c$	9.66 N

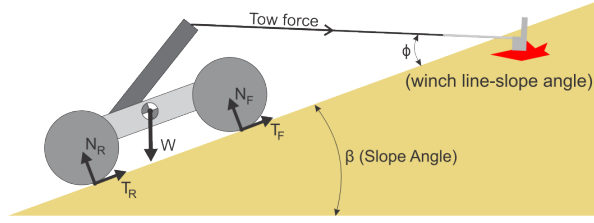


Fig. 6. A free-body diagram of the rover illustrating the net force

### C. Net Force

The net force of a vehicle (drawbar pull force on flat ground) is the sum of the traction, towing, gravitational, and resistive forces acting on it. If the vector component of the vehicle's weight down a given slope is less than the net force, the vehicle can ascend that slope. It is also important to note that on a slope, the vehicle's weight shifts between wheels.

The tow force assists the tractive component of the net force and counteracts load transfer to the rover's rear wheel. Since the magnitude of the tow force depends on the anchor's geometry and not the rover's mass, reducing the rover's mass would allow it to climb a greater slope angle. Since tractive forces are generally proportional to normal load [23], the tow force effectively increases the traction of the front wheel on a slope without increasing the rover's mass.

The net force can be observed from Fig. 6 to be:

$$F_{net} = T_R + T_F + F_{tow} \cos \phi - W \sin \beta \quad (4)$$

This informs us that the net force increases with the tow force, and decreases with the slope angle.

## IV. EXPERIMENTAL RESULTS

### A. Energetics of launch

To explore how symmetry affects the energetics of launch, we tested two different anchors, the nominal anchor used in the device (asymmetric about the rod axis) and one symmetric about the rod axis (Fig. 7). We launched each anchor with the launcher mounted to ground to prevent kick-back and measured the take-off velocity with high-speed video. We plotted the kinetic energy of each anchor,  $\frac{1}{2}mv^2$ , normalized by the initial spring energy  $\frac{1}{2}kx^2 + cx$  (see Section III-B). The results (Fig. 7) show that the symmetric has substantially lower losses than the asymmetric anchor. We believe this is due to flexing of the anchor rod during launch in the asymmetric case, leading to friction with the launcher. Note that the maximum possible efficiency is higher with the asymmetric anchor. This is because the ratio  $\frac{m_{anchor}}{m_{total}}$  is higher for the asymmetric anchor than for the symmetric anchor, which raises the kinetic energy as seen in (1).

### B. Launch distance vs. pullback distance

To experimentally verify our model for launch distance (Section III-B, Equation 3), we launched the symmetrically-headed anchor described in Section II-B horizontally from a height of 0.3 m, with the rear of the launcher pressed against a wall to eliminate recoil. The point at which the head first

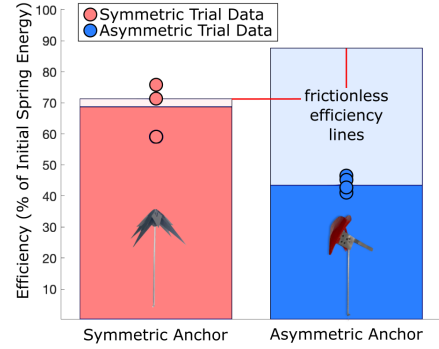


Fig. 7. The launch energy efficiency of the different anchors tested, showing that a symmetric anchor minimizes energy loss.

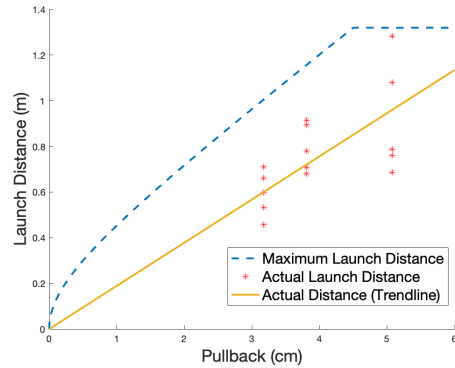


Fig. 8. Launch distance of the asymmetric anchor vs spring pullback distance, compared to the maximum theoretical launch distance from (3).

landed was marked, and its distance from the head's location just before launch was recorded as the launch distance. This distance was recorded at three different pullback distances, ranging from 3.2 cm to 5.1 cm.

### C. Anchoring force vs. angle of attack

To prove that the anchor can achieve the desired performance (providing a high anchoring force at low angles of attack, and a low anchoring force at high angles of attack) the angle-dependent anchoring force of the anchor was measured in dry, unprepared sand at a beach volleyball court. The anchor head was first horizontally dragged 60 cm with the winch line, which submerged it on every trial ( $N=20$ ). It was then pulled with a Mark-10 M3 force gauge at a prescribed angle of attack for either an additional horizontal distance of 60 cm or until it surfaced, and the maximum tensile force was recorded. Note that the anchor does slip somewhat as it is pulled, but it provides anchoring force regardless.

The results shown in Fig. 9 show that the maximum horizontal anchoring force was about 75 N, while the maximum vertical anchoring force was about 15 N, a 5:1 ratio. This angle-dependent force allows the winch to tow the rover at parallel (when the anchor is launched) and reset the anchor at perpendicular (when the rover has reached the anchor).

Although the magnitude of the anchoring force depends on properties of the sand or soil, this angle dependence still

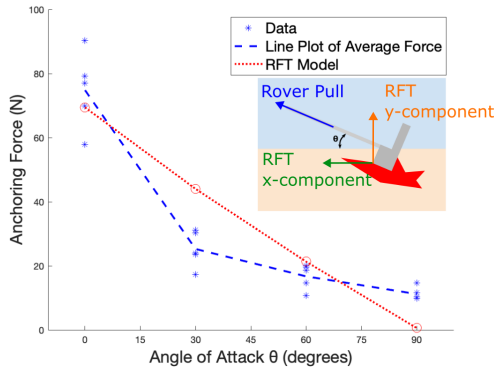


Fig. 9. The anchoring force of the anchor prototype, plotted as a function of the angle of attack of the winching string attached to the anchor. The high force at low angles allows it to anchor, while the low force at high angles allows it to be pulled out of the ground and reset into the launcher. Results follow expected force decrease predicted by resistive force theory (RFT) model.



Fig. 10. The anchor launcher being used to climb a  $17^\circ$  slope of GRC-1 lunar regolith simulant at the NASA Glenn Research Center SLOPE Lab. A) Rover is stuck and cannot climb further. B) Anchor is launched. C) Rover has winched itself up to anchor. D) Anchor is pulled out of sand and resets into launcher.

holds as shown by the resistive force theory model, enabling the system to automatically reset as the rover increases the angle of attack by approaching the buried anchor.

#### D. Launcher testing on a rover in lunar regolith simulant

To demonstrate the utility of the anchor launcher for lunar rovers, we performed slope climbing experiments at the NASA Glenn Research Center Simulated Lunar Operations Laboratory (SLOPE) Lab. The main regolith bin of the SLOPE lab is filled with GRC-1 lunar regolith simulant and has a section of the test bed that can be tilted at a prescribed angle. GRC-1 was designed to recreate the behavior of native lunar regolith in lunar gravity, on Earth in Earth gravity for the study of rover mobility [24].

Fig. 10 and the attached video media [19] show the rover using the anchor launcher to help it climb a  $17^\circ$  slope. The rover approached the slope under the power of its wheels, but could not climb the slope due to slipping and avalanching of the regolith simulant under its wheels. Next, the anchor was launched and the rover’s wheels were driven in tandem

with the winch to pull the rover up the slope, then reset and launched again. In this manner, the rover climbed about 2 m (four body lengths) with three winch launches in 6 minutes.

Due to its low mass, our rover could only climb slopes up to  $15^\circ$  before soil shear failure and avalanching at its wheels prevented forward progress (this avalanching is the failure mode of the anchor). With the help of the anchor launcher, the rover could climb slopes up to  $17^\circ$  without avalanching; higher slopes caused avalanching failure.

## V. CONCLUSION

We have presented a proof-of-concept anchor launcher capable of allowing a planetary rover to independently rescue itself from soft-soil entrapment, even in a scenario where uphill climbing is required. The anchor launcher is able to reset itself and allow the rover to continue moving unimpeded, and/or use the launcher again if needed.

Although effective for our rover experiment, the launch distance for the anchor could be improved. As described in Sec. III, this could be done by decreasing the weight of the carriage, anchor, and spring, as well as increasing the energy in the spring. Furthermore, creating a symmetric anchor with the same anchoring ability as the current asymmetric design would decrease losses, which we believe are due to friction caused by the bending of the asymmetric anchor. Finally, it is possible to reduce the friction as the winch line unspools.

The effectiveness of the anchor in loose soils is another area of future research. With a modified boat anchor, only a 2-degree improvement was seen in slope climbing before the anchor failed. An anchor optimized for loose soils could improve performance. Additionally, for removal from entrapment, the anchor could be aimed at preferable anchoring points (like a mound or stronger soil) for better anchoring.

Other general improvements include designing a system that allows dynamic rotation of the launcher on the rover body; this would allow optimization of launch distance on any slope, simply by changing the angle at which the launcher sits. Comparing climbing power consumption with and without the winch could prove useful. Additionally, one could develop an aiming system integrated with the rover’s vision and path planning systems, or simultaneously use multiple anchors with independently controlled winches to enable complex lateral movements on steep slopes.

Other important considerations for extraterrestrial use include changes in gravity and atmosphere. The anchor’s initial dig into the ground is affected by its weight, which would be lessened in reduced gravity. Additionally, in vacuum, there would be no drag on the anchor, allowing it to fly farther. An anchor optimized to be launched on the Moon may be different than for Earth and require protection against abrasive regolith.

Overall, our self-resetting anchor launcher presents an alternative way to increase rover mobility up steep slopes and rescue them from entrapment.

## REFERENCES

- [1] L. A. Vedeshin, “The first soviet experiments on remote sensing and contact study of the moon (on the 50th anniversary of the moon

- landing of lunokhod 1 self-propelled vehicle),” *Izvestiya.*, vol. 57, no. 12, pp. 1800–1802, 2021–12.
- [2] D. Bickler, “Roving over mars,” *Mechanical Engineering*, vol. 120, no. 04, p. 74–77, Apr 1998. [Online]. Available: <https://asmdigitalcollection.asme.org/memagazineselect/article/120/04/74/367689/Roving-Over-Mars-Operating-Nearly-125-Million-Miles>
- [3] M. Heverly, J. Matthews, J. Lin, D. Fuller, M. Maimone, J. Biesiadecki, and J. Leichty, “Traverse performance characterization for the mars science laboratory rover,” *Journal of Field Robotics*, vol. 30, no. 6, pp. 835–846, 2013. [Online]. Available: <https://onlinelibrary.wiley.com/doi/abs/10.1002/rob.21481>
- [4] J. L. Callas, “Mars Exploration Rover Spirit end of mission report,” 2015. [Online]. Available: <https://hdl.handle.net/2014/45471>
- [5] A. Thoesen and H. Marvi, “Planetary surface mobility and exploration: A review,” *Current Robotics Reports*, vol. 2, no. 3, pp. 239–249, 2021.
- [6] C. Cao, A. Rogg, and A. Tardy, “Actuated suspension tuning characterization of the viper lunar rover,” in *2023 IEEE Aerospace Conference*. IEEE, 2023, pp. 1–11.
- [7] C. Creager, K. Johnson, M. Plant, S. Moreland, and K. Skonieczny, “Push–pull locomotion for vehicle extrication,” *Journal of Terramechanics*, vol. 57, pp. 71–80, 2015.
- [8] S. Yin, W. Wang, L. Hu, Z. Zhu, and Z. Jia, “Attitude control of an all-wheel-drive rover with integrated active suspension system,” in *2023 9th International Conference on Mechatronics and Robotics Engineering (ICMRE)*, 2023, pp. 58–64.
- [9] F. Cordes, F. Kirchner, and A. Babu, “Design and field testing of a rover with an actively articulated suspension system in a mars analog terrain,” *Journal of Field Robotics*, vol. 35, no. 7, pp. 1149–1181, 2018.
- [10] A. Bouton and Y. Gao, “Crawling locomotion enabled by a novel actuated rover chassis,” in *2022 International Conference on Robotics and Automation (ICRA)*, 2022, pp. 8164–8170.
- [11] S. Shrivastava, A. Karsai, Y. O. Aydin, R. Pettinger, W. Bluethmann, R. O. Ambrose, and D. I. Goldman, “Material remodeling and unconventional gaits facilitate locomotion of a robophysical rover over granular terrain,” *Science robotics*, vol. 5, no. 42, p. eaba3499, 2020.
- [12] T. Huntsberger, A. Stroupe, H. Aghazarian, M. Garrett, P. Younse, and M. Powell, “Tressa: Teamed robots for exploration and science on steep areas,” *Journal of Field Robotics*, vol. 24, no. 11–12, pp. 1015–1031, 2007. [Online]. Available: <https://onlinelibrary.wiley.com/doi/abs/10.1002/rob.20219>
- [13] A. Bouloubasis, G. McKee, P. Tolson, O. Tokhi, A. Bouloubasis, G. McKee, and P. Tolson, “Novel concepts for a planetary surface exploration rover,” *The Industrial robot.*, vol. 34, no. 2, pp. 116–121, 2007–03–13.
- [14] P. Abad-Manterola, J. Edlund, J. Burdick, A. Wu, T. Oliver, I. Nesnas, and J. Cecava, “Axel: A minimalist tethered rover for exploration of extreme planetary terrains,” *IEEE Robotics and Automation Magazine*, vol. 16, 12 2009.
- [15] J. J. Page, L. K. Treers, S. Jorgensen, R. Fearing, and H. S. Stuart, “The robustness of tether friction in non-idealized terrains,” *IEEE Robotics and Automation Letters*, vol. 8, no. 1, pp. 424–431, 2023.
- [16] N. Violante-Carvalho, V. D’Avila, H. H. Villena, and A. M. Filippo, “The flying anchor: An original technique for beach profile measurements in the surf zone,” *Journal of Coastal Research*, vol. 36, no. 3, pp. 654–660, 2020.
- [17] R. Dudziak, S. Tuttle, and S. Barraclough, “Harpoon technology development for the active removal of space debris,” *Advances in Space Research*, vol. 56, no. 3, pp. 509–527, 2015.
- [18] S. Völk, S. Ulamec, J. Biele, M. Hecht, P. Lell, J. Fleischmann, S. Althapp, M. Grebenstein, J. A. Nuth, D. C. Wegel, *et al.*, “Development and testing of a pyro-driven launcher for harpoon-based comet sample acquisition,” *Acta Astronautica*, vol. 152, pp. 218–228, 2018.
- [19] “Supplementary video,” 2025. [Online]. Available: <https://www.youtube.com/watch?v=IOJLWEAKmac>
- [20] E. W. Hawkes, C. Xiao, R.-A. Peloquin, C. Keeley, M. R. Begley, M. T. Pope, and G. Niemeyer, “Engineered jumpers overcome biological limits via work multiplication,” *Nature*, vol. 604, no. 7907, pp. 657–661, 2022.
- [21] T. Nakayama, “Range of projectile motion.” [Online]. Available: <http://www.phys.ufl.edu/~nakayama/lec2048.pdf>
- [22] C. Li, T. Zhang, and D. I. Goldman, “A terradynamics of legged locomotion on granular media,” *science*, vol. 339, no. 6126, pp. 1408–1412, 2013.
- [23] K. Yoshida and H. Hamano, “Motion dynamics of a rover with slip-based traction model,” in *Proceedings 2002 IEEE International Conference on Robotics and Automation (Cat. No.02CH37292)*, vol. 3, 2002, pp. 3155–3160 vol.3.
- [24] H. A. Oravec, X. Zeng, and V. M. Asnani, “Design and characterization of grc-1: A soil for lunar terramechanics testing in earth-ambient conditions,” *Journal of Terramechanics*, vol. 47, no. 6, pp. 361–377, 2010.